Measurement of minority carrier diffusion length in p -GaN using electron emission spectroscopy (EES)

Wan Ying Ho, Yi Chao Chow, Shuji Nakamura, Jacques Peretti, Claude Weisbuch, James S Speck

Measurement of Minority Carrier Diffusion Length in *p*-GaN using Electron Emission Spectroscopy (EES)

Wan Ying Ho[1,a)], Yi Chao Chow[1], Shuji Nakamura[1,2], Jacques Peretti[3], Claude Weisbuch,[1,2] and James S. Speck[1]

[1]*Materials Department, University of California, Santa Barbara, California 93106-5050, USA*

[2]*Department of Electrical Engineering, University of California, Santa Barbara, California 93106-5050, USA*

[3]*Laboratoire de Physique de la Matière Condensée, CNRS, Ecole Polytechnique, Institut Polytechnique de Paris, 91120 Palaiseau, France*

[a)]*wanying_ho@ucsb.edu*

Electron Emission Spectroscopy (EES) was performed on metalorganic chemical vapor deposition grown p-n^--n^+ junctions with p-thicknesses ranging from 50 to 300 nm, doped with [Mg] = 3.5×10^{19} cm^{-3}. By measuring the decreasing emitted electron intensity from a cesiated p-GaN surface with increasing p-thickness, we were able to extract the minority carrier diffusion length of electron in p-type GaN, L_e = 26 ± 3 nm. The measured value is in good agreement with literature reported values. The extrapolated electron current at the n^- region – p-GaN interface is in reasonable agreement with the simulated electron current at the interface.

The minority carrier diffusion length is one of the important material properties to be considered in the analysis of a wide variety of semiconductor devices.[1–3] A range of experimental techniques have been implemented for measurement of the carrier diffusion length, such as electron beam induced current (EBIC),[2,4,5] junction-based photocurrent,[6] time resolved four wave mixing, light induced transient grating (LITG),[7,8] surface photo-voltage spectroscopy,[9] and a combination of photoluminescence (PL) spectroscopy and cross-sectional cathodoluminescence (CL) microscopy.[10] In all these techniques, the material of interest was measured with external excitations such as electron or optical beam under zero bias conditions, which is different from the conditions of an electrically active device. In most of the techniques, complicated optics or modelling were required as well. In this study, we report on determination of the electron diffusion length L_e in *p*-type GaN from electrically active p-n^--n^+ junctions using Electron Emission Spectroscopy (EES).

In EES, a device of interest, typically a diode, is introduced into an ultra-high vacuum (UHV) environment.[11–16] The surface of the device (*p*-type region) is then activated to achieve negative electron affinity (NEA) by depositing cesium or other low work function materials on the surface.[17–19] By lowering the vacuum level to below the bulk conduction band minimum (CBM), the probability of electrons near the surface escaping into vacuum is increased. These electrons travel from the *n*-region where they were injected by the external circuit at the *n*-contact. In their journey through the active region and *p*-region, these electrons experience recombination and scattering, altering their energies, momenta, and concentration. By measuring the energy distribution of the emitted electrons, we are able to infer the processes experienced by the electrons. An Auger recombination process will generate hot electrons that can be located in higher energy side valleys,[11,12,14–16,20] while overflow electrons will be detected in the conduction band

minimum (Γ-valley). A simplified schematic of electron overflow in a *p*-*n* junction as measured in the EES is depicted in Fig. 1.

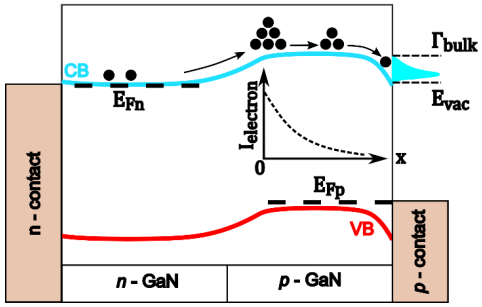

Figure 1: Schematic showing electron overflow in a forward biased *p*-*n* junction, with the relevant energy levels drawn. The electron concentration reduces further away from the junction in the *p*-GaN with a characteristic length known as the minority electron diffusion length. E_{vac} is the vacuum level at the surface of the sample, Γ_{bulk} is the position of the bulk crystal conduction valley minimum (Γ-valley), E_{Fn} and E_{Fp} are the quasi-Fermi levels of the electrons in *n*-GaN and holes in *p*-GaN, respectively.

The (0001) GaN p-n^--n^+ epitaxial structures were grown by metal-organic chemical vapor deposition (MOCVD) on a single side polished (0001) sapphire substrate in the following order: 2 µm thick unintentionally-doped (UID)-GaN buffer layer, 2 µm *n*-type GaN:Si layer ([Si] = 4×10^{18} cm^{-3}), 1 µm UID-GaN drift region, either 50, 75, 150, 200, or 300 nm GaN:Mg ([Mg] = 3.5×10^{19} cm^{-3}), and a highly doped 15 nm *p*-contact layer ([Mg] = 3×10^{20} cm^{-3}). The UID region was designed to be thick to ensure low forward leakage current such that the injected carriers pass through the junction instead of leakage pathways.[21] The highly doped p-contact layer is necessary to achieve ohmic contact to the *p*-GaN. Aside from the *p*-layer thickness, the samples were grown under identical conditions to ensure that the *n*- and UID-GaN are nominally identical. The order of growths were randomized to decouple systematic growth variation effects. The *p*-thicknesses were determined by calibrating growth rates using X-ray diffraction, where thickness fringes were used for thickness determination on a calibration sample. Since it was reported that the diffusion

length is highly dependent on the material quality and doping concentration,[22] for thorough comparison we measured the full width at half maximum of the (0002) and $(20\bar{2}1)$ X-ray diffraction peaks on these samples, which are 220 and 350 arcsec, respectively, giving an estimated threading dislocation density (TDD) of 5×10^8 cm^{-2}.[23] The doping concentrations reported were determined using Secondary Ion Mass Spectroscopy (SIMS).

For each sample, a single EES device of honeycomb pattern of area 0.22 mm^2 was made, comprising of an array of 4602 exposed hexagonal *p*-GaN with an apothem of 2.5 μm separated by 2 μm wide 30 nm Pd/ 300 nm Au metal strips.[13] The ratio of exposed *p*-GaN to metal area for the device is 45:55. The sample was cleaned using HCl and acidic piranha before introduction into an UHV EES system as described elsewhere.[11] A submonolayer of Cs was deposited (cesiation) using a SAES Getters cesium source while monitoring photoexcited electrons emitted from *p*-GaN, with which negative electron affinity (NEA) was confirmed when the photoemitted current increased and reached a maximum.[11] The escape probability of an electron at the *p*-GaN surface is affected by the position of the vacuum level E_{vac} and the condition of the cesiated surface. Since it is a function of the emitting surface, photoemission quantum yield (Y) measurements were performed on an exposed area of *p*-GaN with no metal coverage using a calibrated focused monochromatic 355 nm beam from an Energetiq Laser Driven Light Source (LDLS^{TM}) EQ-99 passed through a monochromator, and the photoemitted electrons were collected using a 90 V biased wire.

EES was performed with the devices biased under pulsed mode in the dark, with variable duty cycles, 100% to 5%, for injection currents ranging from 1 to 45 mA corresponding to average current densities ranging from 0.45 to 20.0 A cm^{-2}, respectively. The injection currents and duty cycles were chosen to be low to avoid self-heating without sacrificing signal-to-noise ratio, and to

ensure that the junction voltage is below the built-in voltage, which is calculated using $V_{BI} \approx \frac{E_G}{q} + \frac{k_B T}{q} \ln\left(\frac{N_D N_A}{N_C N_V}\right)$, where E_G is the bandgap of GaN, N_D and N_A are the donor and acceptor concentration in *n*- and *p*-GaN, respectively, and N_C and N_V are the effective density of the conduction band and valence band states, respectively. For the measured doping, the built-in voltage is calculated to be 3.33 V. The samples were electrically similar with a maximum voltage difference of 0.27 V at 20 A cm^{-2} between samples of different thicknesses after accounting for series resistances (see Fig. 2 (a)). Circular Transmission Length measurements (CTLMs) yielded *p*-contact and *n*-contact specific contact resistivities of $7.2 \times 10^{-4}\ \Omega\ \mathrm{cm}^{-2}$ and $5.7 \times 10^{-5}\ \Omega\ \mathrm{cm}^{-2}$, respectively. The ideality factors of the diodes, η were extracted from the linear regime of the current – voltage (I – V) curves using the equation:

$$\ln(I) = \ln(I_S) + \frac{qV}{\eta k_B T} \tag{1}$$

where I_S is the reverse saturation current. η ranges from 1.73 to 2.27 for these diodes, indicating deviation from ideal diode behavior due to presence of recombination centers in the middle of the junction. Capacitance – Voltage (C-V) measurements as shown in Fig. 2 (b) based on Hilibrand and Gold indicated that the UID-region has a net average electron concentration:

$$\bar{n}(\mathrm{UID}) = \frac{2}{q\varepsilon \frac{d(1/C^2)}{dV}} \tag{2}$$

in the low 10^{15} cm^{-3},[24] where ε is the permittivity of GaN. Hence the UID region is essentially a lightly *n*-doped region due to incorporation of oxygen impurities, a shallow donor.[25–27] SIMS measurements supported the CV data, indicating that the oxygen concentration in the UID region is below detection limit at < 10^{16} cm^{-3}.

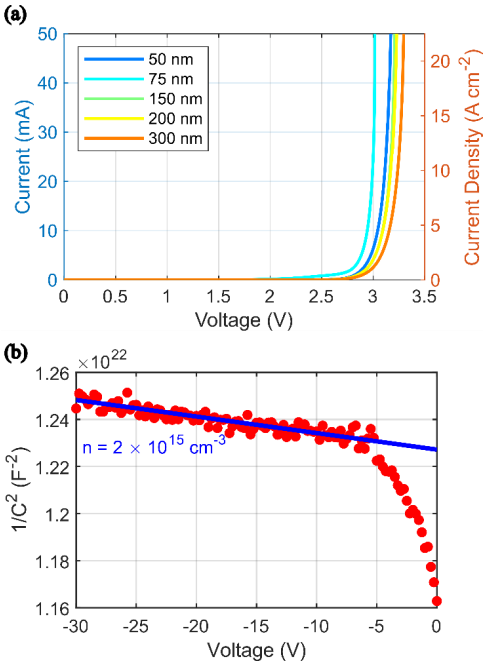

Figure 2: (a) Current – Voltage (I-V) curves for the different diodes measured. The curves shown are corrected for series resistances. The corresponding average current density of the diodes are included. The ideality factors of the diodes are extracted from the linear regime in ln(I) vs. V plots far from turn-on. (b) Capacitance – Voltage (C-V) measurements indicated that the UID-region has net electron concentration in the low 10^{15} cm^{-3}.

The energy of the emitted electrons was measured referenced to the Fermi level of the *p* contact using a Comstock AC-901 spherical sector electrostatic analyzer operated in constant pass energy mode with an energy resolution of 90 meV.[12] A corresponding set of pulsed and continuous wave (CW) measurements were performed using the 90 V collection wire without energy resolution to quantify the collection efficiency of the energy analyzer and Faraday cup.

With increasing diode current, there was an increased voltage drop across the metal-semiconductor interface that shifted the measured energy of electrons emitted from the semiconductor surface to higher values.[12,13] Inversely, by comparing the energy shift with the

applied diode current (or voltage) we can extrapolate the energy shift to expected zero diode current which should correspond to the bulk CBM. The high energy thresholds of peaks resolved in the energy distribution curves (EDCs) were extracted from the zero-intercept of the positive slopes in the derivatives of the EDCs (DEDCs).[28–30]

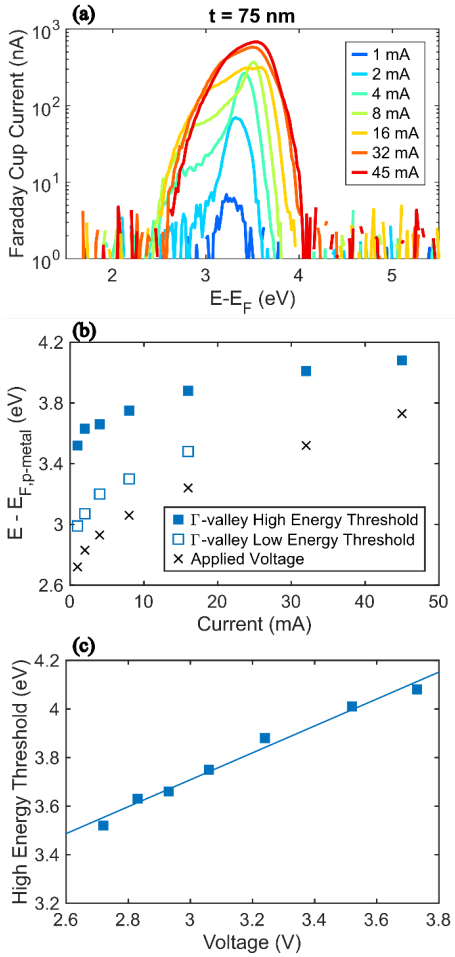

Figure 3: The measured energy distribution curves (in terms of Faraday cup current) shown in (a) for the $d_{p-\mathrm{GaN}} = 75$ nm sample at different currents, exhibiting one distinct peak. The peak has a high energy threshold of ~3.5 eV at 0.45 A cm^{-2} (1 mA) as shown for the $d_{p-\mathrm{GaN}} = 75$ nm sample in (b), which corresponds to the Γ-valley CBM in GaN and increases with increasing applied diode voltage in (c).

The measured energy distribution curves (EDCs) for the $d_{p-\mathrm{GaN}} = 75$ nm sample at different diode currents are shown in Fig. 3 (a), where a main distinguishable peak is observed for each EDC. The extracted high energy thresholds for this peak increase with increasing applied diode voltage as shown in Figs. 3 (b) and (c), indicating its origin to be from the semiconductor. The high energy threshold at 0.45 A cm^{-2} is found to be 3.52 eV above the Fermi level, which corresponds to the bulk CBM (Γ-valley) of GaN. The obtained bulk valley minimum is higher than the true value due to additional small voltage drops from the UHV stage clips to the sample p-surface, which is indicated by a corresponding shift in the low energy threshold of the Γ-valley peak with injected current as depicted in Fig. 3 (b).

The collected currents with and without energy resolution, $I_{emitted}$, after correction for photoemission quantum yield, Y (as described below) for various diode currents are shown in Fig. 4. The electron current increases by four orders of magnitude with diminished top-layer thickness.

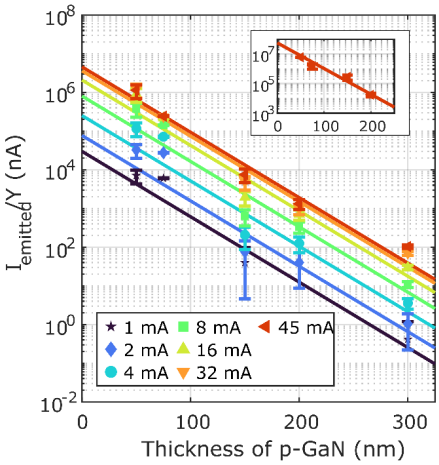

Figure 4: The total collected current ($I_{emitted}$) after correction by quantum yield (Y), of electroemitted electrons from the 90 V biased collection wire for different diode currents decreases with increasing p-GaN thicknesses. The inset shows a corresponding integrated intensity from the energy distribution curve obtained using the analyzer and Faraday cup system for diode current of 45 mA (the horizontal and vertical axes for the inset have the same units as the main figure).

The electron current reaching the surface is governed by the minority carrier diffusion equation. From there, the minority carrier diffusion length, L_e in the p layer is obtained by solving the diffusion equation in the form of:

$$\frac{d^2 n_p}{dx^2} = \frac{n_p}{D_n \tau_n} = \frac{n_p}{L_e^2} \tag{3}$$

where n_p is the minority carrier (electrons) concentration in p-GaN, $D_n = \sqrt{k_B T \mu_n / q}$ the diffusion coefficient at temperature T for electron mobility μ_n, τ_n the lifetime of the electrons, while k_B and q have their usual meanings of Boltzmann constant and electron charge. After applying relevant boundary conditions, this equation has solutions of the form:

$$n_p(x) = n_p(x = 0) e^{-\frac{x}{L_e}}$$

where $n_p(x = 0)$ is the electron density at the injection interface between the UID depleted region and the top *p*-GaN layer. From this expression, we deduce the one of I_{emitted}, the emitted electron current from the activated surface of a *p*-*i*-*n* junction with a *p*-doped layer of thickness d:

$$I_{\text{emitted}}(d) = I_e P_{\text{esc}} e^{-\frac{d}{L_e}} \tag{4}$$

where I_e is the electron current at the injection interface between the UID depleted region and *p*-GaN interface and P_{esc} is the escape probability of the electrons from the emitting surface. P_{esc} can be different for the different samples because it depends on the surface activation and on the recombination velocity of photoelectrons at the surface. It can be determined from the measurement of the photoemission quantum yield, Y, according to the following equation:

$$Y(\lambda) \approx P_{esc}(1 - R_\lambda)\frac{\alpha_\lambda L_e}{1 + \alpha_\lambda L_e} \tag{5}$$

where R_λ and α_λ are, respectively, the reflectivity of the sample surface and the absorption coefficient for $\lambda = 355$ nm, chosen to be just above the optical bandgap.[31,32] Note that the photoemission quantum yield expression has no explicit dependence on the *p*-GaN thickness, *d*, when L_e is smaller than 1/α, and than d, which will be confirmed below.

Then, L_e can be determined from the slope of the dependence of I_{emitted}/Y on the p-GaN layer thickness *d*:

$$\ln\left[\frac{I_{\text{emitted}}(d)}{Y_\lambda}\right] = -\frac{x}{L_e} + \ln\left(I_e \frac{1 + \alpha_\lambda L_e}{(1 - R_\lambda)\alpha_\lambda L_e}\right) \tag{6}$$

The photoemission quantum yield measured at 355 nm ranges from 0.3% to 1.3% for the series. The total collected currents for measurements with energy resolution is obtained by summing over the entire EDC. Normalizations for the pulsed diode currents are applied to both collection wire currents and EDCs by dividing by their corresponding duty cycles. All measurements yielded good

fits to equation 6 (Pearson's coefficients, $R = -0.98$). Performing least square fits across all currents in Fig. 4 yielded diffusion lengths of 25 nm from the EDC measurements and 26 nm from the total current collection wire.[33] Note that these values are indeed smaller than $1/\alpha$, which is 100 nm for $\alpha = 10^5$ cm^{-1}, and d.[34]

We can analyze further the data in Fig. 4: the slopes are of course the diffusion length, and the separation between the lines giving data for different injected electron currents represent the resulting different injected electron currents at the interface of UID-GaN and *p*-GaN where $x = 0$. It is clear from the *y*-intercepts of the straight lines in Fig. 4 that the injected electron current at $x = 0$ is not linearly proportional to the diode current, spanning two orders of magnitude for diode current range of 1 to 45 mA. Since the differences may arise due to the presence of hole current as the EES system only detects electrons and not holes, to analyze the *y*-intercept of the fits – the expected electron current collected at zero *p*-GaN thickness in these *p-i-n* diodes, I_e – we must first calculate the injected electron current at the interface of the UID-GaN and *p*-GaN. Using a 1D Poisson-drift-diffusion solver, the current – voltage ($J - V$) characteristics of these devices were simulated.[35–37] The non-radiative Shockley-Read-Hall (SRH) lifetime of the electrons, τ_{nonrad} in *p*-GaN was taken to be 60 ps while τ_{nonrad} in UID-GaN was varied from 3 ns to 50 ns. τ_{nonrad} of holes in the UID-GaN was taken to be same as that of electrons in UID-GaN. Current crowding effects were accounted for using analytical solutions for circular apertures to approximate the lateral junction current density profile of hexagonal apertures.[38] Further details of the simulation are included in the supplementary material (also see references therein).[13,22,37,39]

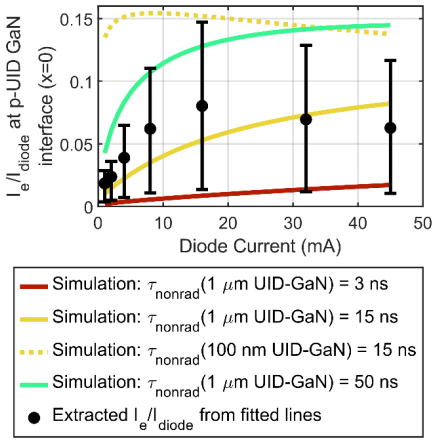

Figure 5: Dependence of the simulated fraction of electron current injected from the UID-GaN into the *p*-GaN region on the supplied diode current with non-radiative carrier lifetimes in the UID-GaN ranging from 3 ns to 50 ns. The simulated current has been corrected for current crowding effects and aperture to metal area ratio, while the experimental data obtained from the *y*-intercepts of lines fitted in Fig. 4 had been corrected for additional loss in the highly doped *p*-contact layer.[38]

The simulated fraction of current injected into *p*-GaN from UID-GaN as electrons, I_e/I_{diode} is plotted in Fig. 5. I_e/I_{diode} is found to be varying with injected current, varying from 1.0% for 1 mA to 8.2% for 45 mA for non-radiative lifetime of electrons in the UID-GaN, τ_{nonrad} of 15 ns, assumed constant for different carrier densities. The fraction of electrons injected into *p*-GaN from UID-GaN reduces as expected for smaller τ_{nonrad}. This is due to the long journey taken by electrons through the thick UID-GaN, where scattering and recombination take place. This is supported by simulations for a short 100 nm thick UID-GaN region with otherwise identical parameters, where larger I_e/I_{diode} were obtained. After accounting for the minority electron loss due to diffusion in the highly doped 15 nm thick *p*-contact region, the experimental I_e/I at $x = 0$ agrees in general with the simulated I_e/I_{diode} for τ_{nonrad} of 15 ns. Despite the small differences in

trend between experimental data and simulation, it is remarkable that I_e/I_{diode} could be reasonably extracted within factor of 2 using EES.

In the literature, electron diffusion length in *p*-GaN measurements based on EBIC techniques reported a wide range of values from 41 to 200 nm, where larger EBIC acceleration voltages appear to correlate to larger measured values.[2,22,40–42] While larger acceleration voltages probes deeper, depth dependent and cross-sectional EBIC measurements by Celio *et al.* reported consistent L_e of ~41 nm between the two different EBIC methods. The measured L_e values reported here are on the lower end of this range of values and are in reasonable agreement with Celio *et al*. In combined PL and CL measurements,[10] there is complication in using the luminescence intensities due to having two possible sources of carriers generating the luminescence spectrum – by diffusion from the p-GaN or by direct photoexcitation, yielding an L_e value of 93 ± 7 nm. This value is four times larger than our reported value possibly because of a larger diffusion coefficient or longer recombination lifetimes due to the high photoexcitation conditions employed.[10,28–30,38] The photoexcited carrier densities were in excess of 10^{18} cm^{-3} while our measurements are simulated to have electron densities ~ 10^{15} to 10^{17} cm^{-3}, hence our results are consistent with the reported diffusion lengths in literature.

In conclusion, we have measured electrons emitted from a series of *c*-plane GaN *p*-*n*$^-$-*n*$^+$ devices with variable *p*-GaN thicknesses. We have shown that the electrons originate from the CBM of GaN and decrease in intensity with increasing *p*-GaN thickness, yielding minority carrier diffusion length of ~26 nm consistent with literature reported values.

Supplementary Material

The supplementary material discusses the analysis of the extracted current at p-n^- metallurgical junction for different samples. The SIMS profile is also included in the discussion.

Acknowledgements

Support at UCSB was provided by the Solid State Lighting and Energy Electronics Center (SSLEEC); the University of California, Santa Barbara (UCSB) – Collaborative Research of Engineering, Science and Technology (CREST) program; U.S. Department of Energy under the Office of Energy Efficiency & Renewable Energy (EERE) Award Nos. DE-EE0007096 and DE-EE0009691; the Simons Foundation (Grant #s 601952 and 1027114 for JSS and CW, respectively); the National Science Foundation (NSF) RAISE program (Grant No. DMS-1839077 for JSS and CW); and Sandia National Laboratory (Award # 2150283). A portion of this work was performed at the UCSB Nanofabrication facility.

References

[1] H.C. Casey, B.I. Miller, and E. Pinkas, "Variation of minority-carrier diffusion length with carrier concentration in GaAs liquid-phase epitaxial layers," Journal of Applied Physics **44**(3), 1281–1287 (1973).
[2] Z.Z. Bandić, P.M. Bridger, E.C. Piquette, and T.C. McGill, "Electron diffusion length and lifetime in *p* -type GaN," Appl. Phys. Lett. **73**(22), 3276–3278 (1998).
[3] W. Götz, N.M. Johnson, J. Walker, D.P. Bour, and R.A. Street, "Activation of acceptors in Mg-doped GaN grown by metalorganic chemical vapor deposition," Appl. Phys. Lett. **68**(5), 667–669 (1996).
[4] L. Chernyak, A. Osinsky, H. Temkin, J.W. Yang, Q. Chen, and M. Asif Khan, "Electron beam induced current measurements of minority carrier diffusion length in gallium nitride," Appl. Phys. Lett. **69**(17), 2531–2533 (1996).
[5] Z.Z. Bandić, P.M. Bridger, E.C. Piquette, and T.C. McGill, "Minority carrier diffusion length and lifetime in GaN," Appl. Phys. Lett. **72**(24), 3166–3168 (1998).
[6] D. Wee, G. Parish, and B. Nener, "Investigation of the accuracy of the spectral photocurrent method for the determination of minority carrier diffusion length," Journal of Applied Physics **111**(7), 074503 (2012).
[7] T. Malinauskas, R. Aleksiejūnas, K. Jarašiūnas, B. Beaumont, P. Gibart, A. Kakanakova-Georgieva, E. Janzen, D. Gogova, B. Monemar, and M. Heuken, "All-optical characterization of carrier lifetimes and diffusion lengths in MOCVD-, ELO-, and HVPE- grown GaN," Journal of Crystal Growth **300**(1), 223–227 (2007).
[8] E.V. Lutsenko, A.L. Gurskii, V.N. Pavlovskii, G.P. Yablonskii, T. Malinauskas, K. Jarašiūnas, B. Schineller, and M. Heuken, "Determination of carrier diffusion length in MOCVD-grown GaN epilayers on sapphire by optical techniques," Phys. Status Solidi (c) **3**(6), 1935–1939 (2006).
[9] Y. Lin, E. Flitsyian, L. Chernyak, T. Malinauskas, R. Aleksiejunas, K. Jarasiunas, W. Lim, S.J. Pearton, and K. Gartsman, "Optical and electron beam studies of carrier transport in quasibulk GaN," Appl. Phys. Lett. **95**(9), 092101 (2009).
[10] S. Hafiz, F. Zhang, M. Monavarian, V. Avrutin, H. Morkoç, Ü. Özgür, S. Metzner, F. Bertram, J. Christen, and B. Gil, "Determination of carrier diffusion length in GaN," Journal of Applied Physics **117**(1), 013106 (2015).
[11] J. Iveland, L. Martinelli, J. Peretti, J.S. Speck, and C. Weisbuch, "Direct Measurement of Auger Electrons Emitted from a Semiconductor Light-Emitting Diode under Electrical Injection: Identification of the Dominant Mechanism for Efficiency Droop," Phys. Rev. Lett. **110**(17), 177406 (2013).
[12] J. Iveland, M. Piccardo, L. Martinelli, J. Peretti, J.W. Choi, N. Young, S. Nakamura, J.S. Speck, and C. Weisbuch, "Origin of electrons emitted into vacuum from InGaN light emitting diodes," Appl. Phys. Lett. **105**(5), 052103 (2014).
[13] D.J. Myers, K. Gelžinytė, W.Y. Ho, J. Iveland, L. Martinelli, J. Peretti, C. Weisbuch, and J.S. Speck, "Identification of low-energy peaks in electron emission spectroscopy of InGaN/GaN light-emitting diodes," Journal of Applied Physics **124**(5), 055703 (2018).
[14] D.J. Myers, K. Gelžinytė, A.I. Alhassan, L. Martinelli, J. Peretti, S. Nakamura, C. Weisbuch, and J.S. Speck, "Direct measurement of hot-carrier generation in a semiconductor barrier heterostructure: Identification of the dominant mechanism for thermal droop," Phys. Rev. B **100**(12), 125303 (2019).
[15] D.J. Myers, A.C. Espenlaub, K. Gelzinyte, E.C. Young, L. Martinelli, J. Peretti, C. Weisbuch, and J.S. Speck, "Evidence for trap-assisted Auger recombination in MBE grown InGaN quantum wells by electron emission spectroscopy," Appl. Phys. Lett. **116**(9), 091102 (2020).
[16] W.Y. Ho, Y.C. Chow, D.J. Myers, F. Wu, J. Peretti, C. Weisbuch, and J.S. Speck, "Quantitative correlation of hot electron emission to Auger recombination in the active region of *c* -plane blue III-N LEDs," Appl. Phys. Lett. **119**(5), 051105 (2021).
[17] M.C. Benjamin, M.D. Bremser, T.W. Weeks, S.W. King, R.F. Davis, and R.J. Nemanich, "UV photoemission study of heteroepitaxial AlGaN films grown on 6H-SiC," Applied Surface Science **104–105**, 455–460 (1996).
[18] M. Eyckeler, "Negative electron affinity of cesiated p-GaN(0001) surfaces," J. Vac. Sci. Technol. B **16**(4), 2224 (1998).
[19] T.U. Kampen, M. Eyckeler, and W. Mönch, "Electronic properties of cesium-covered GaN(0001) surfaces," Applied Surface Science **123–124**, 28–32 (1998).
[20] W.Y. Ho, A.I. Alhassan, C. Lynsky, Y.C. Chow, D.J. Myers, S.P. DenBaars, S. Nakamura, J. Peretti, C. Weisbuch, and J.S. Speck, "Detection of hot electrons originating from an upper valley at ∼ 1.7 eV above the Γ valley in wurtzite GaN using electron emission spectroscopy," Phys. Rev. B **107**(3), 035303 (2023).
[21] C.A. Robertson, Defect-Mediated Carrier Transport Mechanisms in Vertical GaN p-n Diodes, University of California, Santa Barbara, 2019.

[22] K. Kumakura, T. Makimoto, N. Kobayashi, T. Hashizume, T. Fukui, and H. Hasegawa, "Minority carrier diffusion length in GaN: Dislocation density and doping concentration dependence," Appl. Phys. Lett. **86**(5), 052105 (2005).
[23] C. Lynsky, R.C. White, Y.C. Chow, W.Y. Ho, S. Nakamura, S.P. DenBaars, and J.S. Speck, "Role of V-defect density on the performance of III-nitride green LEDs on sapphire substrates," Journal of Crystal Growth **560–561**, 126048 (2021).
[24] J. Hilibrand, and R.D. Gold, "Determination of the impurity distribution in junction diodes from capacitance-voltage measurements," RCA Rev. **21**, 245–252 (1960).
[25] C.G. Van de Walle, C. Stampfl, and J. Neugebauer, "Theory of doping and defects in III–V nitrides," Journal of Crystal Growth **189–190**, 505–510 (1998).
[26] A.J. Ptak, L.J. Holbert, L. Ting, C.H. Swartz, M. Moldovan, N.C. Giles, T.H. Myers, P. Van Lierde, C. Tian, R.A. Hockett, S. Mitha, A.E. Wickenden, D.D. Koleske, and R.L. Henry, "Controlled oxygen doping of GaN using plasma assisted molecular-beam epitaxy," Appl. Phys. Lett. **79**(17), 2740–2742 (2001).
[27] R.Y. Korotkov, and B.W. Wessels, "Electrical Properties of Oxygen Doped GaN Grown by Metalorganic Vapor Phase Epitaxy," MRS Internet j. Nitride Semicond. Res. **5**(S1), 301–307 (2000).
[28] H.-J. Drouhin, C. Hermann, and G. Lampel, "Photoemission from activated gallium arsenide. I. Very-high-resolution energy distribution curves," Phys. Rev. B **31**(6), 3859–3871 (1985).
[29] J. Peretti, H.-J. Drouhin, and D. Paget, "High-resolution energy analysis of field-assisted photoemission: A spectroscopic image of hot-electron transport in semiconductors," Phys. Rev. B **47**(7), 3603–3619 (1993).
[30] M. Piccardo, L. Martinelli, J. Iveland, N. Young, S.P. DenBaars, S. Nakamura, J.S. Speck, C. Weisbuch, and J. Peretti, "Determination of the first satellite valley energy in the conduction band of wurtzite GaN by near-band-gap photoemission spectroscopy," Phys. Rev. B **89**(23), 235124 (2014).
[31] W.E. Spicer, "Photoemissive, Photoconductive, and Optical Absorption Studies of Alkali-Antimony Compounds," Phys. Rev. **112**(1), 114–122 (1958).
[32] W.E. Spicer, "Negative affinity 3–5 photocathodes: Their physics and technology," Appl. Phys. **12**(2), 115–130 (1977).
[33] Chen, Avinadav, "Multiple curve fitting with common parameters using NLINFIT," (2016).
[34] J.F. Muth, J.D. Brown, M.A.L. Johnson, Z. Yu, R.M. Kolbas, J.W. Cook, and J.F. Schetzina, "Absorption Coefficient and Refractive Index of GaN, AlN and AlGaN Alloys," MRS Internet j. Nitride Semicond. Res. **4**(S1), 502–507 (1999).
[35] H.K. Gummel, "A self-consistent iterative scheme for one-dimensional steady state transistor calculations," IEEE Trans. Electron Devices **11**(10), 455–465 (1964).
[36] D.N. Arnold, G. David, D. Jerison, S. Mayboroda, and M. Filoche, "Effective Confining Potential of Quantum States in Disordered Media," Phys. Rev. Lett. **116**(5), 056602 (2016).
[37] C.-K. Li, M. Piccardo, L.-S. Lu, S. Mayboroda, L. Martinelli, J. Peretti, J.S. Speck, C. Weisbuch, M. Filoche, and Y.-R. Wu, "Localization landscape theory of disorder in semiconductors. III. Application to carrier transport and recombination in light emitting diodes," Phys. Rev. B **95**(14), 144206 (2017).
[38] W.B. Joyce, and S.H. Wemple, "Steady-State Junction-Current Distributions in Thin Resistive Films on Semiconductor Junctions (Solutions of $\nabla^2 v = \pm e^v$)," Journal of Applied Physics **41**(9), 3818–3830 (1970).
[39] D.J. Myers, Electron Emission Spectroscopy of III-N Semiconductor Devices, University of California, Santa Barbara, 2019.
[40] K.C. Celio, A.M. Armstrong, A.A. Talin, A.A. Allerman, M.H. Crawford, G.W. Pickrell, and F. Leonard, "Carrier Diffusion Lengths in Continuously Grown and Etched-and-Regrown GaN Pin Diodes," IEEE Electron Device Lett. **42**(7), 1041–1044 (2021).
[41] S. Guermazi, A. Toureille, C. Grill, and B. El Jani, "Extended generation profile - E.B.I.C model application in the case of a PN junction," Eur. Phys. J. AP **9**(1), 43–49 (2000).
[42] J.C. Gonzalez, K.L. Bunker, and P.E. Russell, "Minority-carrier diffusion length in a GaN-based light-emitting diode," Appl. Phys. Lett. **79**(10), 1567–1569 (2001).
[43] T. Malinauskas, K. Jarasiunas, M. Heuken, F. Scholz, and P. Brückner, "Diffusion and recombination of degenerate carrier plasma in GaN," Phys. Status Solidi (c) **6**(S2), (2009).
[44] G. Bemski, "Lifetime of Electrons in p -Type Silicon," Phys. Rev. **100**(2), 523–524 (1955).
[45] J.S. Blakemore, "Lifetime in p -Type Silicon," Phys. Rev. **110**(6), 1301–1308 (1958).
[46] G.B. Abdullaev, Z.A. Iskender-Zade, E.A. Dzhafarova, and V.E. Chelnokov, "Study of Electron Lifetime in p-Si," phys. stat. sol. (b) **21**(1), 423–429 (1967).

PLEASE CITE THIS ARTICLE AS DOI: 10.1063/5.0150029